Competitive Diffusion-Influenced Reaction of a Reactive Particle with Two Static Sinks

V. M. Bluett and N. J. B. Green*

Department of Chemistry, King's College London, Strand, London WC2R 2LS, U.K.

Received: November 28, 2005; In Final Form: February 3, 2006

An investigation into the kinetics of reaction between a diffusing particle and a system of two static spherical sinks is presented. The backward diffusion equation is solved for the probability of reaction with each sink, using both absorbing and radiation boundary conditions. The rate constants for each reaction are also calculated. The reactivity of the sinks is shown to be subadditive, and if the sinks are asymmetric the less reactive sink is more strongly affected by the competition. Competitive effects are found to be modeled adequately by using effective reaction radii. The IRT method is shown to have serious defects for such a system because of the correlation of the two sinks. An application to the reaction of OH radicals with thymidine is presented.

1. Introduction

The attack of free radicals on organic molecules is an area of great importance in understanding the mechanisms of radiation damage. In this respect, hydroxyl radicals formed by the radiolysis of water are of most interest. The reactions of hydroxyl radicals with organic molecules are generally rather undiscriminating and are close to diffusion control.[1] The molecule attacked may contain several reactive sites, which may be sufficiently close to one another for the concentration gradients of the radicals around each site to overlap and interfere with one another so that the reactivity of the sites is not additive. In these circumstances, a curious effect has been observed experimentally: the rate constants for OH attack on thymine and deoxyribose are in a ratio of approximately 3:1,[1] but when the two moieties are linked in the molecule thymidine the ratio becomes approximately 10:1.[2] One interesting question that arises is the extent to which this may be a diffusive competition effect.

A simple model of this system would be two reactive spheres linked together at a fixed separation, one representing the base and the other representing the sugar. The diffusion of the radicals relative to this bispherical system could then be analyzed assuming that the spheres are fixed. This is a crude model of the real thymidine system because both the base and the sugar contain several reactive centers themselves and because the rotational diffusion of the thymidine molecule is ignored. However, the model does have the virtue of being analytically tractable and can be used to investigate the possibility of competition between the two moieties.

In this paper the steady-state diffusion kinetics are analyzed for this model, with particular emphasis on working out which sphere reacts first. The exact solutions are compared with the predictions of the IRT (independent reaction times) model, in which, for each radical, random reaction times are generated independently for the two spheres from the known radical−sphere distances. The IRT model has proven to be very accurate in modeling competitive radical recombination reactions, where all of the reactive radicals are mobile.

The aims of this study are to estimate the magnitude of the competition effect as a function of the intersphere distance, to investigate whether this competition can be described using the IRT method, and to investigate whether the competition of partly diffusion-controlled reactions is affected by the use of effective reaction spheres, that is, by replacing a radiation boundary at a realistic encounter distance with an absorbing boundary at a smaller reaction distance and the same overall reactivity.

In Section 2 the backward diffusion equation with two spherical sinks is set up and solved for the probability that a diffusing particle will react with one sink before the other. The problem is formulated and solved analytically in bispherical coordinates, with totally absorbing boundaries and with partially reflecting boundaries. Section 3 discusses the well-known relationship between reaction probability and rate constant, which can be combined with the results of Section 2 to give rate constants for the reaction with either sink. Section 4 deals with the special case of a reactive sphere in the presence of a reactive or partially reflecting plane, which is a limiting case. Section 5 applies the IRT approximation to the two-sphere problem. Because of the relative simplicity of the model system, the IRT method also gives an explicit analytic solution. In Section 6 the two methods are applied to a variety of systems and compared with one another. It is demonstrated that the IRT method is not capable of dealing with the competition between the two spheres. Finally, in Section 7 the results are applied to thymidine to assess whether the competition between the base and sugar moieties can explain the apparent anomaly in the experimental rate constants.

2. General Solution for Two Fixed Spherical Sinks

The problem of the steady-state rate coefficient for diffusion-controlled reaction of a species distributed homogeneously in space with two fixed spherical sinks has been solved previously by Samson and Deutch.[3] Samson and Deutch consider the total reactivity of the system of two spheres. However, it is of interest to differentiate between the two spheres, especially where they represent distinguishable chemical reaction sites, and for such a system it is more convenient to start by considering the different (but related) problem of a single radical diffusing in the presence of two spherical sinks. This approach requires the probability that the particle reacts with each of the sinks separately as a function of its initial position. In the case of diffusion-controlled reaction of the two spheres, a formal solution to this problem has been presented by Sano.[4]

Suppose that the two sinks are labeled 1 and 2. The probability of reacting with sphere 1 is the probability that the particle reacts with sphere 1 before sphere 2 (if it would have

10.1021/jp0568881 CCC: $33.50
Published on Web 03/17/2006

reacted with sphere 2 at all). This probability obeys the steady-state backward diffusion equation.[5]

$$\nabla_0^2 \mathscr{P}_1 = 0 \tag{1}$$

in which the Laplacian operator differentiates with respect to the initial coordinates of the particle.

The bispherical coordinate system is the natural coordinate system for solving this problem.[6] These are defined as follows:

$$z = \frac{a \sinh \mu}{\cosh \mu - \cos \eta} \tag{2}$$

$$x = \frac{a \sin \eta \cos \phi}{\cosh \mu - \cos \eta} \tag{3}$$

$$y = \frac{a \sin \eta \sin \phi}{\cosh \mu - \cos \eta} \tag{4}$$

The variable μ can take any real value. Surfaces of constant μ are spheres of radius $a/|\sinh \mu|$, centered at (0, 0, a coth μ). In the limits $\mu \rightarrow \pm\infty$ the isosurfaces shrink toward the foci $z = \pm a$. The parameter a is known as the interfocal distance. The surface $\mu = 0$ is the xy plane. Any system of two nonintersecting spheres can be arranged so that each spherical boundary is a fixed value of the coordinate μ. The variable η can take values between 0 and π. Surfaces of constant η are formed by rotating the positive part of a circle of radius $a/\sin \eta$ and center (0, 0, a cotη) about the z axis, together with its reflection in the xy plane. All isosurfaces of the variable η intersect on the circle $x^2 + y^2 = a^2$. The variable ϕ represents the usual longitude angle, as in spherical polar coordinates. Sections through typical isosurfaces of μ and η have cylindrical symmetry about the z axis, and sections of typical isosurfaces taken through the xz plane are shown in Figure 1.

2.1. Transformation into Bispherical Coordinates. In the first case to be considered, the two spherical sinks have the same radius, b, and their centers are separated by a distance d ($d > 2b$). The spheres are equidistant from the origin on the z axis. Then the boundaries are at $\mu = \pm\cosh^{-1}(d/2b)$ and the interfocal distance $a = b \sinh |\mu|$.

If the two spheres do not have the same radius, then the interfocal distance, a, must be obtained by solution of the equation

$$d = \sqrt{a^2 + b_1^2} + \sqrt{a^2 + b_2^2} \tag{5}$$

and then $\mu_1 = \sinh^{-1}(a/b_1)$ and $\mu_2 = -\sinh^{-1}(a/b_2)$, where b_1 and b_2 are the two sphere radii.

The permitted space for the diffusion is the whole of space outside the spheres, this is $\mu_2 < \mu < \mu_1$, $0 < \eta < \pi$, and $0 < \phi < 2\pi$. Within this permitted space, a given initial position can be converted to bispherical coordinates using

$$\mu = \tanh^{-1}\left(\frac{2az}{x^2 + y^2 + z^2 + a^2}\right) \tag{6}$$

$$\eta = \cos^{-1}\left(\cosh \mu - \frac{a}{z} \sinh \mu\right) \tag{7}$$

$$\phi = \tan^{-1}(y/x) \tag{8}$$

On the plane $z = 0$ ($\mu = 0$) due care must be taken to obtain the correct limit for η.

2.2. Formal Solution. Following the transformation $F = \sqrt{\cosh\mu - \cos\eta}\,\mathscr{P}_1$, the Laplace equation in bispherical coordinates is transformed to[6]

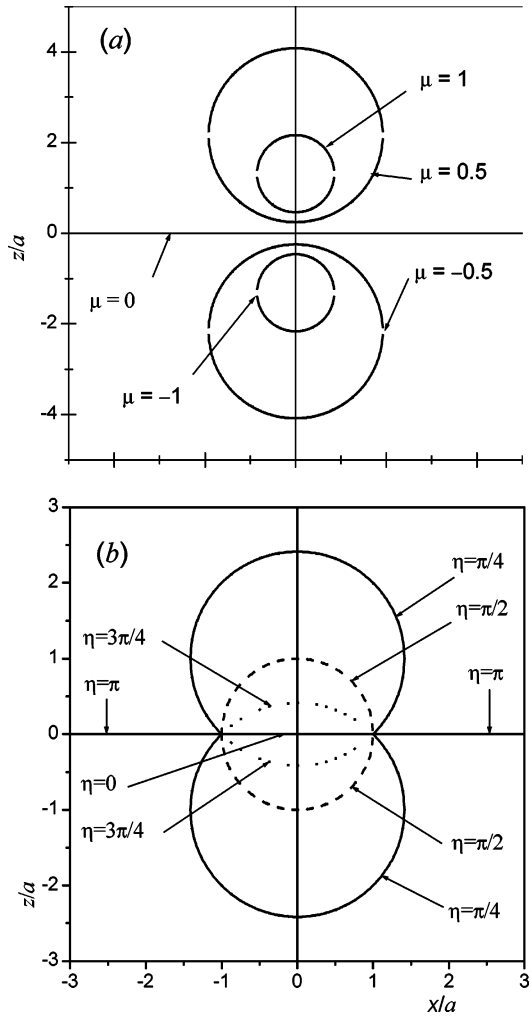

Figure 1. Section through the xz plane of the isosurfaces of the bispherical coordinates. (a) Surfaces of constant μ, (b) surfaces of constant η. The surfaces are obtained by rotating the section about the z axis.

$$\frac{\partial^2 F}{\partial \mu^2} + \frac{1}{\sin \eta} \frac{\partial}{\partial \eta}\left(\sin \eta \frac{\partial F}{\partial \eta}\right) + \frac{1}{\sin^2 \eta} \frac{\partial^2 F}{\partial \phi^2} - \frac{1}{4} F = 0 \tag{9}$$

The separation of variables is standard and, taking into account the cylindrical symmetry of the system around the z axis, the general solution can be written

$$\mathscr{P}_1 = \sqrt{(\cosh \mu - \cos \eta)} \sum_{n=0}^{\infty} (A_n e^{(n+1/2)\mu} + B_n e^{-(n+1/2)\mu}) P_n(\cos \eta) \tag{10}$$

where P_n denotes the Legendre polynomials.

The arbitrary constants A_n and B_n must be found from the boundary conditions. The next sections consider in turn various boundary conditions of interest.

2.3. Totally Absorbing Boundaries. The simplest case to solve is that of two totally absorbing boundaries and is of interest because it describes the situation in which reaction with both spheres is diffusion-controlled.

The appropriate boundary conditions are

$$\mathscr{P}_1(\mu_1) = 1 \tag{11}$$

$$\mathscr{P}_1(\mu_2) = 0 \tag{12}$$

The interpretation of these boundary conditions is that a particle starting in contact with sink 1 is certain to hit sphere 1 before sphere 2, and a particle starting in contact with sink 2 is certain not to hit sink 1 before sink 2.

Substituting $\mu = \mu_1$ into the general solution and using the first boundary condition

$$\frac{1}{\sqrt{(\cosh \mu_1 - \cos \eta)}} = \sum_{n=0}^{\infty} (A_n e^{(n+1/2)\mu_1} + B_n e^{-(n+1/2)\mu_1}) P_n(\cos \eta) \tag{13}$$

But the LHS can also be expanded as a series of Legendre polynomials, giving

$$\sqrt{2} \sum_{n=0}^{\infty} e^{-(n+1/2)|\mu_1|} P_n(\cos \eta) = \sum_{n=0}^{\infty} (A_n e^{(n+1/2)\mu_1} + B_n e^{-(n+1/2)\mu_1}) P_n(\cos \eta) \tag{14}$$

Because the Legendre polynomials are linearly independent, the coefficient of each P_n on the LHS must be equal to the corresponding coefficient on the RHS, giving

$$\sqrt{2} e^{-(n+1/2)|\mu_1|} = A_n e^{(n+1/2)\mu_1} + B_n e^{-(n+1/2)\mu_1} \tag{15}$$

Similarly, the other boundary condition gives the relationship

$$0 = A_n e^{(n+1/2)\mu_2} + B_n e^{-(n+1/2)\mu_2} \tag{16}$$

Solving for A_n and B_n yields the solution

$$\mathscr{P}_1 = \sqrt{2(\cosh \mu - \cos \eta)} \sum_{n=0}^{\infty} e^{-(n+1/2)\mu_1} \frac{\sinh\left(\left(n+\frac{1}{2}\right)(\mu - \mu_2)\right)}{\sinh\left(\left(n+\frac{1}{2}\right)(\mu_1 - \mu_2)\right)} P_n(\cos \eta) \tag{17}$$

This solution has been obtained previously by Sano.[4] The probability of hitting sphere 2 before sphere 1 follows by symmetry.

The probability that the particle hits one or other of the two spheres is $\mathscr{P}_1 + \mathscr{P}_2$ and can also be found by solving the backward equation with boundary values of 1 on both spheres. The probability that the particle escapes without hitting either sphere is $1 - (\mathscr{P}_1 + \mathscr{P}_2)$.

2.4. Partially Reflecting Boundaries. *2.4.1. Probability of Reacting with Sphere 1 First.* The probability of hitting sphere 1 first is found by solving eq 1 subject to the following boundary conditions:[7]

$$D(\nabla \mathscr{P}_1)_{\mu_2} = v_2 \mathscr{P}_1(\mu_2) \tag{18}$$

$$D(\nabla \mathscr{P}_1)_{\mu_1} = v_1(1 - \mathscr{P}_1(\mu_1)) \tag{19}$$

where v_1 and v_2 are the "reaction velocities" of spheres 1 and 2, respectively, and D is the diffusion coefficient of the OH radical. The reaction velocity is a parameter that describes the reactivity of each species in contact with the OH radical. The natural units for such a parameter are those of velocity.[8]

Substituting the general solution (eq 10) into the first boundary condition yields, after a certain amount of algebra

$$\mathbf{S}(\mu_2, v_2)\mathbf{A} - \mathbf{S}(-\mu_2, -v_2)\mathbf{B} = 0 \tag{20}$$

where $\mathbf{A}$ and $\mathbf{B}$ are vectors with elements A_i and B_i, $i = 0, 1, 2, \ldots$ $\mathbf{S}(\mu, v)$ is an infinite tridiagonal matrix whose elements are

$$\mathbf{S}_{n,n-1}(\mu, v) = e^{(n+1/2)\mu}\left[-\frac{D}{2} n e^{-\mu}\right] \quad n = 1, 2, 3 \ldots \tag{21}$$

$$\mathbf{S}_{n,n+1}(\mu, v) = e^{(n+1/2)\mu}\left[-\frac{D}{2}(n+1)e^{\mu}\right] \quad n = 0, 1, 2 \ldots \tag{22}$$

$$\mathbf{S}_{n,n}(\mu, v) = e^{(n+1/2)\mu}\left[\frac{D}{2}\sinh \mu + D\left(n+\frac{1}{2}\right)\cosh \mu - av\right] \quad n = 0, 1, 2 \ldots \tag{23}$$

Similar working to the above leads from the second boundary condition to the following relation between coefficients of $\mathbf{A}$ and $\mathbf{B}$

$$\mathbf{S}(\mu_1, -v_1)\mathbf{A} - \mathbf{S}(-\mu_1, v_1)\mathbf{B} = \mathbf{c} \tag{24}$$

where the vector $\mathbf{c}$ has elements $c_n(\mu, v) = av\sqrt{2}e^{-(n+1/2)\mu}$, $n = 0, 1, 2, \ldots$

Equations 20 and 24 may be combined into the following single matrix equation whose solution yields the values of the coefficients A_n and B_n

$$\begin{pmatrix} \mathbf{S}(\mu_2, v_2) & -\mathbf{S}(-\mu_2, -v_2) \\ \mathbf{S}(\mu_1, -v_1) & -\mathbf{S}(-\mu_1, v_1) \end{pmatrix}\begin{pmatrix} \mathbf{A} \\ \mathbf{B} \end{pmatrix} = \begin{pmatrix} 0 \\ \mathbf{c}(\mu_1, v_1) \end{pmatrix} \tag{25}$$

Vectors $\mathbf{A}$ and $\mathbf{B}$ are found by solving this equation. Although they are both infinite vectors, the general solution given by eq 10 converges quickly, and only the first 50 or so elements of each vector are required to obtain $\mathscr{P}_1$ to a high degree of accuracy from any starting point of the diffusing radical.

2.4.2. Probability of Reacting with Sphere 2 First. The general solution for $\mathscr{P}_1$ given by eq 10 applies equally to $\mathscr{P}_2$, the probability of hitting sphere 2, with the different set of boundary conditions

$$D(\nabla \mathscr{P}_2)_{\mu_1} = -v_1 \mathscr{P}_2(\mu_1) \tag{26}$$

$$D(\nabla \mathscr{P}_2)_{\mu_2} = -v_2(1 - \mathscr{P}_2(\mu_2)) \tag{27}$$

Comparison with equations 18 and 19 shows that the constants A_n and B_n in the general solution (eq 10) may be found by replacing μ_1 by μ_2, μ_2 by μ_1, v_1 by $-v_2$ and v_2 by $-v_1$ in matrix eq 25 to yield the following matrix equation

$$\begin{pmatrix} \mathbf{S}(\mu_1, -v_1) & -\mathbf{S}(-\mu_1, v_1) \\ \mathbf{S}(\mu_2, v_2) & -\mathbf{S}(-\mu_2, -v_2) \end{pmatrix}\begin{pmatrix} \mathbf{A} \\ \mathbf{B} \end{pmatrix} = \begin{pmatrix} 0 \\ \mathbf{c}(\mu_2, -v_2) \end{pmatrix} \tag{28}$$

Solving for $\mathbf{A}$ and $\mathbf{B}$ gives the required coefficients in the general solution.

2.5. Mixed Boundary Types. Sections 2.3 and 2.4 show how to determine $\mathscr{P}_1$ and $\mathscr{P}_2$ when both spheres have similar boundary types, either both totally absorbing or both partially absorbing. This Section considers a different situation in which one of the spheres has a totally absorbing boundary and the other has a partially reflecting boundary. Let sphere 1 ($\mu = \mu_1$

> 0) have an absorbing boundary and sphere 2 ($\mu = \mu_2 < 0$) have a partially reflecting boundary with characteristic velocity v_2.

2.5.1. Probability of Reacting with Sphere 1 First. As before, $\mathscr{P}_1$ is defined to be the probability of hitting sphere 1 first.

The boundary conditions are

$$\mathscr{P}_1(\mu_1) = 1 \tag{29}$$

$$D(\nabla\mathscr{P}_1)_{\mu_2} = v_2\mathscr{P}_1(\mu_2) \tag{30}$$

The first boundary condition leads to the following relationship between the constants A_n and B_n in the general solution.

$$\sqrt{2} = A_n e^{(2n+1)\mu_1} + B_n \tag{31}$$

The second boundary condition is identical to that given in eq 18 of Section 2.4.1. and employing the notation of that Section, leads to the following relationship between A_n and B_n

$$\mathbf{S}(\mu_2, v_2)\mathbf{A} - \mathbf{S}(-\mu_2, -v_2)\mathbf{B} = 0 \tag{32}$$

Combining eqs 31 and 32 into a single matrix equation

$$\begin{pmatrix} \mathbf{S}(\mu_2, v_2) & -\mathbf{S}(-\mu_2, -v_2) \\ \mathbf{J}(\mu_1) & \mathbf{I} \end{pmatrix}\begin{pmatrix} \mathbf{A} \\ \mathbf{B} \end{pmatrix} = \begin{pmatrix} 0 \\ \mathbf{d} \end{pmatrix} \tag{33}$$

where $\mathbf{J}(\mu)$ is a diagonal matrix with elements

$$J_{n,n}(\mu) = e^{(2n+1)\mu} \quad n = 0, 1, 2, ... \tag{34}$$

$\mathbf{I}$ is the identity matrix, and $\mathbf{d}$ is a vector defined as

$$\mathbf{d}_n = \sqrt{2} \quad n = 0, 1, 2 ... \tag{35}$$

Solving eq 33 for $\mathbf{A}$ and $\mathbf{B}$ yields the constants A_n and B_n in the general solution for $\mathscr{P}_1$.

2.5.2. Probability of Reacting with Sphere 2 First. In a very similar way the coefficients in the solution for $\mathscr{P}_2$ obey the equations

$$\begin{pmatrix} \mathbf{J}(\mu_1) & \mathbf{I} \\ \mathbf{S}(\mu_2, -v_2) & -\mathbf{S}(-\mu_2, v_2) \end{pmatrix}\begin{pmatrix} \mathbf{A} \\ \mathbf{B} \end{pmatrix} = \begin{pmatrix} 0 \\ \mathbf{c}(\mu_2, -v_2) \end{pmatrix} \tag{36}$$

3. Rate Constant Evaluation

Having obtained expressions for the probability of reacting with either sphere, starting from any given point outside the spheres, it is necessary to work out how to translate these results into rate constants.

Consider first the general situation in which a static particle, A, is surrounded in a region of volume V by a sea of reactive particles B of uniform concentration c. The time-dependent rate constant is defined in the usual way as

$$k(t) = -\frac{1}{c}\frac{d}{dt}(\ln \Omega(t)) \tag{37}$$

where $\Omega(t)$ represents the time-dependent survival probability of A. Assuming that the number of B's in the volume V has a Poisson distribution, then it is well-known that[9−12] the survival probability of A is given by

$$\Omega(t) = \exp(-c\int_V W(\mathbf{r}, t)\, d\mathbf{r}) \tag{38}$$

where $W(\mathbf{r}, t)$ is the probability that a geminate AB pair with a B particle at initial position vector $\mathbf{r}$ will have reacted by time t. Combining eqs 37 and 38, the following expression for the rate constant is obtained:

$$k(t) = \int_V \frac{\partial W}{\partial t}\, d\mathbf{r} \tag{39}$$

Using the backward diffusion equation, we can write this equation as

$$k(t) = D\int_V \nabla^2 W\, d\mathbf{r} \tag{40}$$

where D is the diffusion coefficient of a B particle. Applying Gauss's theorem, this volume integral is equivalent to the surface integral

$$k(t) = -D\int \nabla W\, d\mathbf{S}_a \tag{41}$$

where S_a is the surface of particle A. The *steady-state* rate constant is given by

$$k = -D\int \nabla W_A\, d\mathbf{S}_a \tag{42}$$

where $W_A(\mathbf{r})$ is the probability that a particle B, which is initially at the point with position vector $\mathbf{r}$, *ever* reacts with A. No assumption has been made about the shape of the surface of A, and the ensuing analysis is made easier by recognizing that, because the system is in a steady state, eq 42 may equivalently be written as

$$k = -D\int_{r\epsilon S_c} \nabla_r W_A\, d\mathbf{S}_c \tag{43}$$

where S_c is any closed surface (for simplicity, a sphere) containing A. Now, imagine a sphere of radius b ($b < c$) which also completely encloses A, then

$$W_A(\mathbf{r}) = \int_{r'\epsilon S_b} W_b(\mathbf{r},\mathbf{r}')W_A(\mathbf{r}')\, d\mathbf{r}' \tag{44}$$

where $W_b(\mathbf{r},\mathbf{r}')$ is the probability that a particle with position vector $\mathbf{r}$ outside a sphere of radius b first hits that sphere at the point with position vector $\mathbf{r}'$.

Combining eqs 43 and 44, the steady-state rate constant is given by

$$k = -D\int_{r\epsilon S_c} \nabla_r \int_{r'\epsilon S_b} W_b(\mathbf{r},\mathbf{r}')\, W_a(\mathbf{r}')\, d\mathbf{r}'\, d\mathbf{S}_c \tag{45}$$

Changing the order of integration

$$k = -D\int_{r'\epsilon S_b} W_a(\mathbf{r}')\int_{r\epsilon S_c} \nabla_r W_b(\mathbf{r},\mathbf{r}')\, d\mathbf{S}_c\, d\mathbf{r}' \tag{46}$$

It is a standard result of electrostatics[13] that

$$W_b(\mathbf{r},\mathbf{r}') = \frac{r^2 - b^2}{4\pi b|\mathbf{r}' - \mathbf{r}|^3} \tag{47}$$

and hence

$$k = \frac{D}{b}\int_{r'\epsilon S_b} W_A(\mathbf{r}')\, d\mathbf{r}' \tag{48}$$

This equation provides the link between the calculation of a probability and the evaluation of the rate constant for reaction with one of the two spheres. An imaginary sphere of radius b is constructed to surround the two reactive spheres. The

probability of reacting with a particular sphere starting from a given point on the large sphere is found using the methods derived in Section 2. The integral around the surface of the enclosing sphere is evaluated numerically to provide an estimate of the steady-state rate constant for reaction with the reactive sphere.

The interpretation of this equation is that it represents the rate constant for hitting the large sphere times the probability that a diffusing radical started at a random point on the surface of the sphere hits the target (the first hit position on the sphere is distributed uniformly).

4. One Spherical Sink and One Plane

Having solved the diffusion equation for two static spheres, the related problem of a static sphere close to a plane is now considered. The competition for a diffusing particle between a plane and a sphere could have applications in, for example, corrosion. There is a choice of two methods for solving the problem: (1) use the results of Section 2 with $\mu_2 = 0$ so that the second sphere is infinitely large and effectively becomes the *xz* plane or (2) employ the *method of images*. Each method will be considered in turn.

4.1. Limiting Case of Two Spheres. The probability of reaction with either the sphere or the plane may be calculated in precisely the same manner as described in Section 2 but with the provision that $\mu_2 = 0$. However, the calculation of a steady-state rate constant is meaningless in this case because no steady state is ever reached when one of the reacting surfaces is of infinite extent, and it is obviously not possible to find an enclosing surface.

If the sphere and plane are both absorbing, eq 17 may be used with $\mu_2 = 0$ to find the probability of hitting the sphere. Hence

$$\mathscr{P}_s = \sqrt{2(\cosh\mu - \cos\eta)} \sum_{n=0}^{\infty} e^{-(n+1/2)\mu_1} \frac{\sinh\left(\left(n+\frac{1}{2}\right)\mu\right)}{\sinh\left(\left(n+\frac{1}{2}\right)\mu_1\right)} P_n(\cos\eta) \quad (49)$$

Similarly, $\mathscr{P}_p$, the probability of hitting the plane first may be obtained by substituting $\mu_2 = 0$ into the solution for $\mathscr{P}_2$ from Section 2.3 to give

$$\mathscr{P}_p = \sqrt{2(\cosh\mu - \cos\eta)} \sum_{n=0}^{\infty} \frac{\sinh\left(\left(n+\frac{1}{2}\right)(\mu_1 - \mu)\right)}{\sinh\left(\left(n+\frac{1}{2}\right)\mu_1\right)} P_n(\cos\eta) \quad (50)$$

Both of these series are absolutely convergent. However, although eq 49 converges quickly for all values of μ, the same is not true for eq 50, which converges slowly, its terms changing sign in a slow oscillation. The convergence is slowest for starting points close to the plane. However, the reactive particle cannot escape completely; that is, it must react with either the plane or the sphere. It therefore follows that the probability of hitting the plane is simply given by $1 - \mathscr{P}_s$. The proof of this is as follows. Adding equations 49 and 50 and simplifying

$$\mathscr{P}_s + \mathscr{P}_p = \sqrt{2(\cosh\mu - \cos\eta)} \sum_{n=0}^{\infty} e^{-(n+1/2)\mu} P_n(\cos\eta) \quad (51)$$

Using the generating function of Legendre polynomials, this simplifies to

$$\mathscr{P}_s + \mathscr{P}_p = \frac{\sqrt{2(\cosh\mu - \cos\eta)}e^{-\mu/2}}{\sqrt{1 - 2e^{-\mu}\cos\eta + e^{-2\mu}}} = 1 \quad (52)$$

It is also possible to accelerate the convergence of the slowly converging series by a number of methods.[14,15] However, it is not necessary to use any of these because of the rapidly converging series for the complement.

The same method can be applied to the case where one or both boundaries are partly reflecting. Again, the series for the probability of reaction with the sphere converges much faster than that for the plane, but the latter probability is simply the complement of the former.

4.2. Method of Images. The method of images provides a simple alternative way of approaching the same problem and is examined in this Section for two different boundary types.

4.2.1. Absorbing Sphere and Plane. Suppose the absorbing sphere $\mu = \mu_1$ has its center on the *z* axis. The plane $z = 0$ is also an absorbing boundary. A reactive particle is placed somewhere in the region of space between the plane and the surface of the sphere. To find the probability that the diffusing particle reacts with the sphere, a second sphere (an *image* sphere) of equal radius to the first is placed behind the plane with its center on the *z* axis and with bispherical coordinate $\mu = -\mu_1$. The absorbing plane is now removed to leave the two identical absorbing spheres.

The probability of hitting each sphere is found using the methods described in Section 2.3. Now, any trajectory that ends on the image sphere must have passed through the plane $z = 0$. However, the trajectories that end on the object sphere divide into two classes: those that pass through $z = 0$ and those that hit the sphere before passing through $z = 0$. By symmetry, the probability that a trajectory passing through $z = 0$ subsequently hits the object sphere is the same as the probability that it hits the image sphere. Hence, the probability of hitting the object sphere without passing through the plane $z = 0$, and hence the probability of hitting the sphere when the absorbing plane $z = 0$ has been replaced, is given by

$$\mathscr{P}_{sphere} = \mathscr{P}_{object} - \mathscr{P}_{image} \quad (53)$$

Because the reactive particle must eventually hit either the plane or the sphere, the probability of hitting the plane is given by $1 - \mathscr{P}_{sphere}$.

4.2.2. Absorbing Sphere and Reflecting Plane. If the plane $z = 0$ is totally reflecting, then the probability of hitting the absorbing sphere is increased. Again an image sphere of equal radius to the object sphere is introduced on the other side of the plane. Now, any trajectory that passes through $z = 0$ and hits the image sphere would, in the presence of the reflecting plane have reflected off the plane and hit the object sphere. Thus, the probability of hitting the sphere when in the presence of the reflecting plane is given by

$$\mathscr{P}_{sphere} = \mathscr{P}_{object} + \mathscr{P}_{image} \quad (54)$$

$\mathscr{P}_{\text{object}}$ and $\mathscr{P}_{\text{image}}$ correspond to $\mathscr{P}_1$ and $\mathscr{P}_2$ in Section 2.3. Clearly, the probability of reaction with the plane is zero.

5. Independent Reaction Times Approximation

The independent reaction times (IRT) approximation is a central approximation of the theory of multibody diffusion kinetics that enables explicit solutions to be obtained. This approximation is implicit in the Smoluchowski theory of the diffusion-controlled rate coefficient. It has also proved very successful in systems containing small clusters of reactive particles, such as radiation tracks.[16−19] Because some exact solutions are now available for three particles, in the case where two of the particles are stationary, it is of interest to use them to test the IRT approximation for systems of this type. These are likely to be the worst possible cases for the approximation because the two fixed sinks ensure that correlations between the interparticle distances persist throughout the evolution of the system.

The first case considered is that of full diffusion-controlled reaction for both sinks, and subsequently the case of partially diffusion-controlled reaction will be dealt with.

5.1. Full Diffusion Control. If the particle has an initial position where the distances to the two spheres (of radii b_1 and b_2) are r_1 and r_2, respectively, then according to the IRT approximation the probability that sphere 1 is hit before sphere 2 is given by the integral

$$\mathscr{P}_1^{\text{IRT}} = \int_0^\infty f(r_1, b_1, t)(1 - F(r_2, b_2, t))\, \mathrm{d}t \qquad (55)$$

where f is the density of the time for the particle to hit sphere 1 in the absence of sphere 2, and $1 - F$ is the probability that the particle has not yet hit sphere 2 by time t in the absence of sphere 1.

$$f(r_1, b_1, t) = \frac{b_1}{\sqrt{4\pi Dt^3}} \frac{r_1 - b_1}{r_1} \mathrm{e}^{-(r_1-b_1)^2/4Dt} \qquad (56)$$

$$F(r_2, b_2, t) = \frac{b_2}{r_2} \operatorname{erfc}\left(\frac{r_2 - b_2}{\sqrt{4Dt}}\right) \qquad (57)$$

Making the change of variable $u = t^{-1/2}$ brings this integral into a standard form[20]

$$\mathscr{P}_1^{\text{IRT}} = \frac{b_1}{r_1}\left(1 + \frac{b_2}{r_2}\left(\frac{2}{\pi}\tan^{-1}\left(\frac{r_2 - b_2}{r_1 - b_1}\right) - 1\right)\right) \qquad (58)$$

An equivalent expression for the probability of hitting sphere 2 before sphere 1 follows by symmetry.

5.2. Partial Diffusion-Control. The well-known distribution function of the reaction time for a partially diffusion-controlled reaction with a spherical sink[7,21] can be expressed as a function of two dimensionless variables, both of which depend on time

$$W(r, t) = \frac{a}{r}\frac{k_a}{k_a + k_D}\{\operatorname{erfc}(y) - \mathrm{e}^{x^2+2xy}\operatorname{erfc}(x + y)\} \qquad (59)$$

where r is the initial separation of the pair, a is the encounter distance, k_a is the finite rate coefficient for reaction on encounter (radiation boundary condition), and k_D is the steady-state Smoluchowski rate constant; the two dimensionless variables are

$$y = \frac{r - a}{\sqrt{4D't}} \qquad (60)$$

and

$$x = \frac{(k_a + k_D)\sqrt{D't}}{k_D a} \qquad (61)$$

The method of Section 5.1 for finding the probability of reacting with either sphere is impractical to use in this case because of the difficulty of finding an explicit form for the integral. Instead, the IRT simulation method is employed to evaluate the integral by a Monte Carlo method.

A random reaction time is generated for reaction with each of the two spheres to find the probability that a diffusing particle started at some point reacts with sphere 1. In each case the time is generated from the geminate reaction time distribution function, that is, ignoring the presence of the other sphere. If the time for reaction with sphere 1 is smaller than that for sphere 2, then the particle reacts with sphere 1, and vice versa. If both reaction times are infinite, then the particle escapes. The process is repeated many times (typically 100 000) to simulate the probability with acceptable random error. This procedure must be repeated for every starting position of the diffusing particle.

The method for generating a random time for reaction with a sphere will be described in a separate paper. The trajectory can be decomposed into two parts. The first part is the diffusion of the particle up to the time at which the sphere is hit for the first time. The second part is the trajectory from the first hit to the reaction. The reaction time is the sum of the times that the particle spends on each part of the trajectory.

Generating the time to the first hit on the sink is straightforward. The required probability distribution function is given by

$$F(r, a, t) = \frac{a}{r}\operatorname{erfc}\frac{r - a}{\sqrt{4Dt}} \qquad (62)$$

and the hit time can therefore be generated from this distribution by the inversion method, as for fully diffusion controlled reactions.[22]

Once a hit has occurred, the distribution function of the time from the hit to the reaction is obtained by substituting $r = a$ in eq 59

$$W(a, t) = \frac{k_a}{k_a + k_D}\{1 - \mathrm{e}^{x^2}\operatorname{erfc}(x)\} \qquad (63)$$

Times are sampled from this probability distribution by an exact composition method, which is summarized as follows.

1. Generate a uniform random number U_1 between 0 and 1.

2. If U_1 is greater than $k_a/(k_a + k_D)$ then reaction never takes place.

3. Otherwise generate a normally distributed random variable with mean 0 and standard deviation $\sqrt{2}$. Let Y be the absolute value of this random variable.

4. Generate a second uniform random number U_2, and let $X = -(\ln U_2)/Y$. This procedure generates an exponentially distributed random variable with mean $1/Y$.

5. Let $T = (Xa)^2/D'$. T is a random variable with the desired probability distribution function.

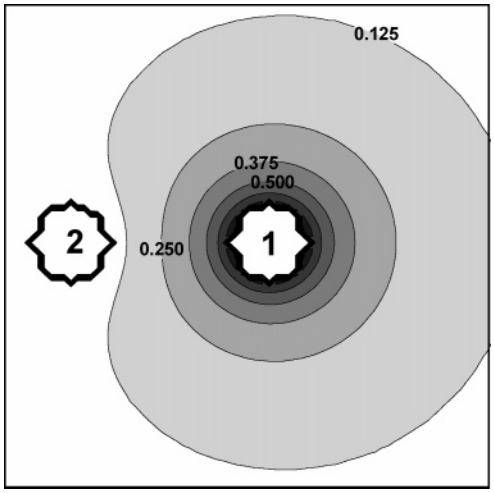

Figure 2. Contour plot of the probability of hitting sphere 1 in a system of two identical absorbing spheres separated by three diameters.

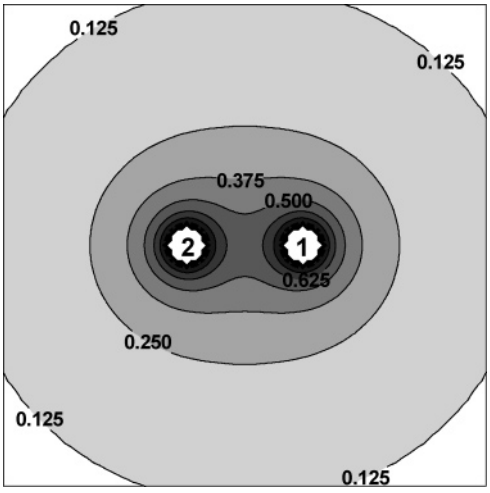

Figure 3. Contour plot of the probability of hitting either sphere in a system of two identical absorbing spheres separated by three diameters.

The proof of this algorithm will be presented elsewhere. The algorithm is straightforward to program, and it has the great attraction of being an exact representation. Previous methods relied on the numerical inversion of the distribution function.[23]

6. Results

The key objective of this paper is to investigate the effect of competition between two proximal reactive species, or reactive sites on the same species, for a diffusing reactive particle. Each reactive site is modeled as a sphere so that the system is tractable to an analytic treatment. The first stage is to calculate the probability of reaction with each sphere as a function of the starting point of the diffusing particle. The next stage is to translate these probabilities into a rate constant for each sphere. This will permit quantification of the extent to which one sphere shields reactivity from the other.

6.1. Reaction Probabilities. *6.1.1. Exact Solutions.* Consider two static spheres whose centers are on the *z* axis; the origin lies at a convenient point between the two spheres. The sphere in the positive region of the *z* axis will be referred to as sphere 1 and the other as sphere 2. A diffusing particle may react with either sphere. One or both spheres may be assigned an absorbing boundary or, alternatively, each sphere may have a finite reaction rate on encounter with this particle. The probability of reaction with a particular sphere may be calculated from the exact solutions in Section 2, or subject to the IRT approximation, as described in Section 5.

As a first example, consider the case of two fully absorbing spheres of equal size, whose centers are separated by three spherical diameters. Because of the cylindrical symmetry of the problem it is only necessary to consider diffusing particles started in the *xz* plane. Figure 2 shows a contour plot of the probability of reaction with sphere 1. In agreement with intuition, it is seen that as the starting position of the particle approaches the surface of sphere 1 the probability approaches 1. However, as the starting position approaches the surface of sphere 2, the probability of reacting with sphere 1 approaches zero. Figure 3 shows the probability of hitting *either* sphere, the complement of the escape probability. The symmetry seen in the plot reflects the fact that the spheres are identical. There is a vast amount of information contained in these figures, far more than is detectable experimentally. The connection with experiment is made by translating the probabilities into a rate constant by the method described above in Section 3. Results for rate constants are discussed in Section 6.2. below.

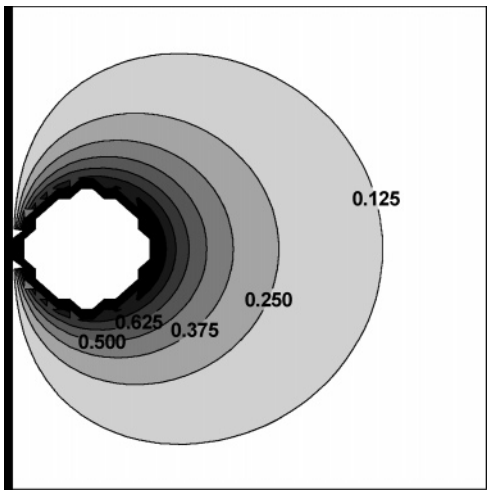

Figure 4. Contour plot of the probability of reaction with an absorbing sphere in the presence of an absorbing plane.

A second example concerns the case of an absorbing sphere in the vicinity of an absorbing plane. The sphere has its center on the positive *z* axis and the plane is the surface $z = 0$. A reactive particle starts its journey in some region of the *xz* plane outside the sphere and with positive *z* coordinate. Figure 4 shows a contour plot of the probability that the diffusing particle reacts with the sphere (rather than the plane) as a function of its starting position. The calculations were carried out using the method described in Section 4. As expected, the plot is symmetric about the *z* axis, and the probability approaches unity as the starting position of the diffusing particle approaches the sphere. The probability distribution shown here cannot be developed into a steady-state rate constant for reaction with either surface. This is because the concentration distribution around the plane is purely transient. Because the sphere is close to the surface of the plane, no steady state can develop around the sphere.

Before looking at rate constant calculations for two spheres of finite reactivity, it is important to assess the accuracy of the IRT approximation when applied to the problem of two static sinks.

6.1.2. Comparison of IRT Calculations with Exact Solutions. The IRT method of calculating reaction probabilities has been described in Section 5. It is an approximate method, and it is of interest to see whether it can be used to good approximation in a system comprising two static sinks. The critical approxima-

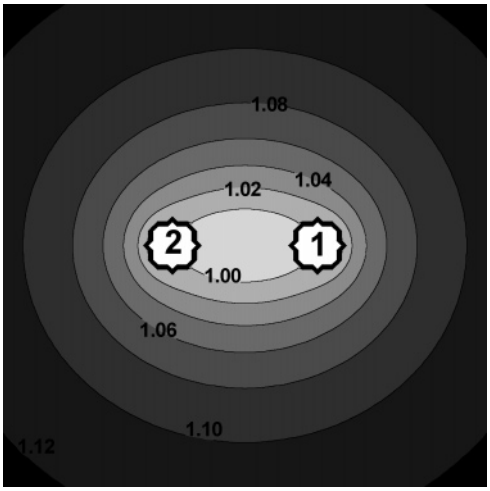

Figure 5. Contour plot of the ratio of the IRT to the exact reaction probability for reaction with either sphere in a system of two identical absorbing spheres separated by three diameters.

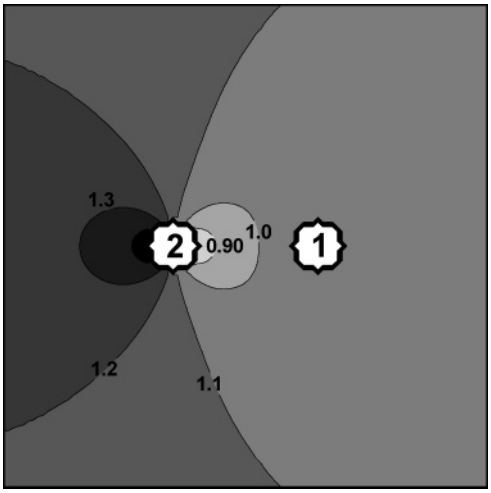

Figure 6. Contour plot of the ratio of the IRT to exact probabilities of hitting sphere 1 in a system of two identical absorbing spheres separated by three diameters.

tion of the IRT method as applied here should be emphasized: no account is taken of the spatial correlation of the two sinks except through their initial distances from the diffusing particle.

To test the IRT approximation, we performed IRT probability calculations for the system of two reactive spheres described in the Section above. Figure 5 shows the ratio of the total reaction probabilities obtained by the IRT method to those obtained by the exact method. It is apparent that the IRT method overestimates the total reaction probability for virtually all starting positions considered. The relative error, typically 10%, increases as the initial distance from the two spheres increases. The exception to this general conclusion is in the region of space between the two spheres, where the reaction probability is slightly underestimated.

An explanation for these contrasting features follows. The IRT method takes account of the initial distance of the diffusing particle from each of the two static sinks; however, it does not take account of their precise relative positions and effectively calculates an average reaction probability over all possible configurations of the two spheres consistent with the initial distances. The configurations in which the two sinks are close together only constitute a small and atypical part of this average. Of all the possible relative positions of the two sinks conditional on these distances, the configuration in which they are side by side presents the greatest possibility for escape for a particle starting a very long way from both particles. This is because trajectories that make for sphere 1 from a large distance are also heading in the direction of sphere 2 and vice versa. By ignoring the strong positive correlation of the two distances as the particle diffuses, the IRT method leads to an overestimate of the reaction probability. The same argument can be applied, but with diminishing importance, as the particle starting position approaches the two spheres. However, if the particle starts in the region between the two spheres, the situation is reversed: the actual configuration now represents the worst possible case for escape for the given distances, and as the particle diffuses the two distances are negatively correlated. The same argument explains why the IRT method underestimates the total reaction probability.

Figure 6 shows the ratio of the probabilities of hitting sphere 1, as calculated by both methods. In the region around sphere 1 the IRT method gives a good estimate of the probability $\mathscr{P}_1$, whereas for initial positions close to sphere 2 there are significant errors: between the spheres this is an underestimate

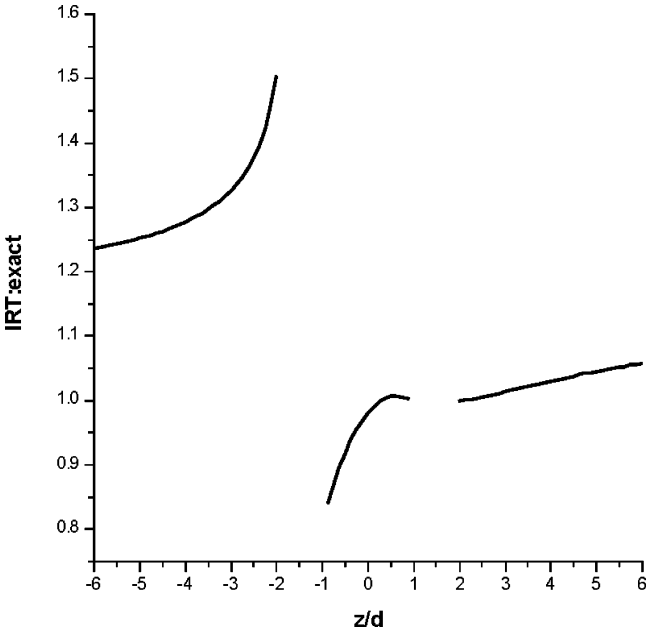

Figure 7. Section of Figure 6 along the *z* axis. The abscissa is the *z* coordinate in units of the sphere diameter.

of $\mathscr{P}_1$, whereas on the far side of sphere 2 there is a large overestimate.

To make sense of the inaccuracies, Figure 7 focuses on a section of the contour plot taken along the *z* axis. It is observed that as the initial position of the particle approaches sphere 2 from the left the ratio increases significantly. This is easy to understand because, from a position on the far side of sphere 2 and close to its surface, a large number of trajectories that would end up on sphere 1 in the absence of sphere 2 will actually be intercepted by sphere 2 first. Because the IRT method does not recognize the correlation between the positions of the two sinks, it overestimates the probability of hitting sphere 1. The closer to sphere 2 the reactive particle starts its journey, the larger the overestimate. In contrast, as the initial position of the particle approaches sphere 1 from the right, the ratio decreases toward 1. The explanation is that the closer the particle starts to sphere 1 the less likely it is to hit sphere 2 first because many trajectories that would strike sphere 2 in the absence of sphere 1 are blocked by sphere 1. The IRT result is less affected than in the previous case because the distance to sphere 1 is much

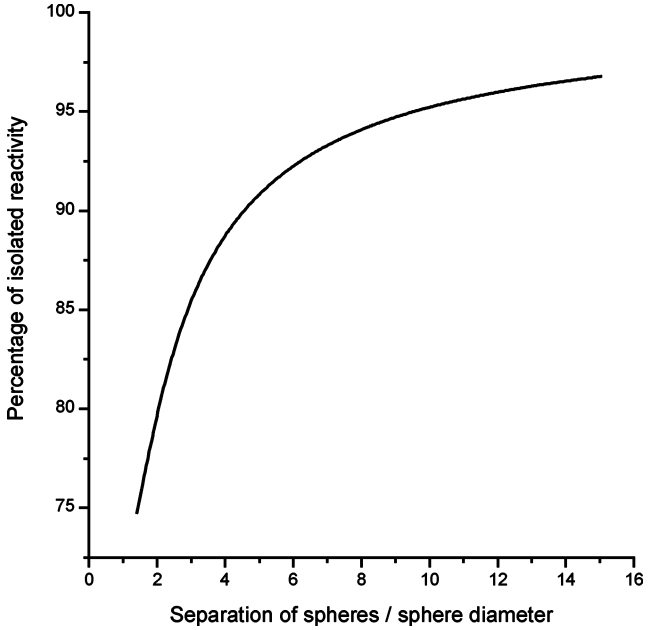

Figure 8. Reduction in relative reactivity of a sphere by competition from a second sphere in a system of two identical absorbing spheres.

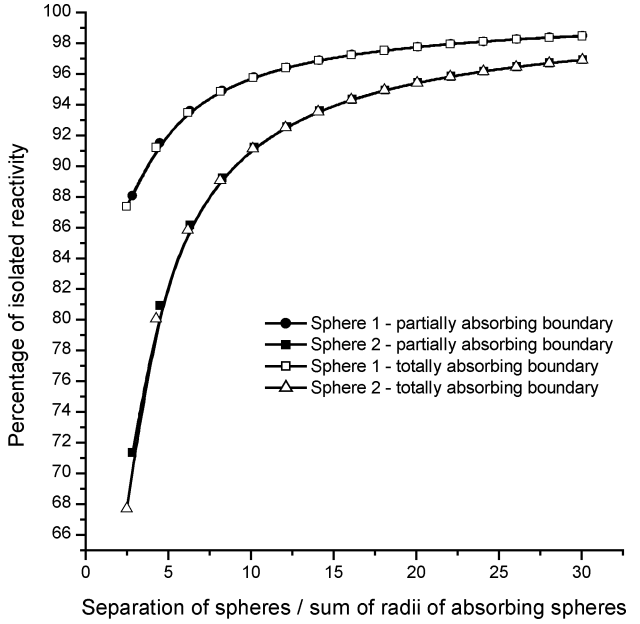

Figure 9. Reduction in reactivity of two spheres relative to the reactivity of each sphere in isolation. Sphere 1 is twice as reactive as sphere 2 when each sphere is in isolation. This difference in reactivity is accounted for in either of two ways: in the first, both spheres are the same size and have partially absorbing boundaries with reactivity parameters chosen such that sphere 1 is twice as reactive as sphere 2; in the second, both spheres have totally absorbing boundaries and sphere 1 has twice the radius of sphere 2.

shorter than the distance to sphere 2 and so in the IRT method most of the trajectories hit sphere 1 first. In the limit where the particle starts in contact with sphere 1 it is trivial that $\mathscr{P}_1 = 1$ in both methods. Of course, this is all superimposed on a background overstatement of both probabilities because of an underestimate of the escape probability.

In the region of the *z* axis between the two spheres, the shape of the ratio is more difficult to justify. However, some insight may be gained from analysis of the similar but simpler case of one-dimensional diffusion between two barriers, which may be found in the appendix.

6.2. Rates. In Section 3, it was shown how to determine a rate constant for reaction of a diffusing particle with either sphere in a system comprising two static proximal spheres. The method is summarized in eq 48.

The importance of the rate constant is that it provides the most convenient link with experiment. In this Section, the method described in the paragraph above is used to evaluate a rate constant for reaction with each sphere. Various boundary types and relative sizes of spheres are considered. Of particular interest is the variation of the rate constant for reaction with a given sphere with the separation of the spheres. Also of interest is the extent to which the relative sizes of two identical spheres affects the ratio of their rate constants.

6.2.1. Two Identical Absorbing Spheres. First two identical absorbing spheres are considered. Figure 8 indicates the rate constant for hitting sphere 1 as a function of the separation between the spheres. This is plotted as a ratio with respect to the rate constant for reaction with a single isolated sphere of the same radius. The total rate constant for the whole system is twice that for hitting each individual sphere. This result agrees with the predictions of Samson and Deutch;[3] in fact, it is straightforward to prove that $\mathscr{P}_1 + \mathscr{P}_2$ is identical to the concentration distribution derived by Samson and Deutch. When the spheres are almost touching, the rate constant for reaction with each sphere is some 25% lower than that of an isolated sphere of the same size. A substantial reduction is to be expected because the second sphere acts to protect the first from many of the trajectories that would otherwise react with it. As the separation increases, there is a corresponding increase in the rate constant for hitting each sphere because the protective effect of the neighboring sphere diminishes. Once the separation reaches 15 spherical diameters, the rate constant is only about 3% less than that of the isolated sphere. The effect of competition beyond this distance is negligible.

6.2.2. Two Spheres of Different Reactivities. This Section considers competition between two spheres of different reactivities. The example considered is one in which sphere 1 is twice as reactive as sphere 2 when each sphere is in isolation. In the example, the difference in reactivity is accounted for in either of two ways: in the first, both spheres have totally absorbing boundaries and the radius of sphere 1 is twice the radius of sphere 2; in the second, both spheres have partially absorbing boundaries and are of equal size but their reaction velocities are assigned in such a way that sphere 1 has twice the reactivity of sphere 2. In the latter case, the parameters are chosen so that each sphere has the same reactivity as the corresponding sphere in the totally absorbing treatment. Figure 9 shows, for each case, the reactivity of each sphere as a percentage of its reactivity in isolation, expressed as a function of the separation between the spheres. It is evident that the competition effect is essentially independent of whether the difference in reactivity is modeled using a reactivity parameter and a realistic radius or diffusion control with an effective radius. The only differences arise at very small separations between the spheres because the effective spheres can be unphysically close to one another.

At all separations there is a reduction in reactivity of each sphere, which diminishes as the separation increases. The reactivity of the less reactive sphere is more affected by the presence of the other sphere. This result can be interpreted in terms of the diffusing particle "bouncing off" or missing the less reactive sphere and being picked up by the more reactive sphere before it returns. Figure 10 shows the variation of the ratio of rate constants with separation. At very short separations

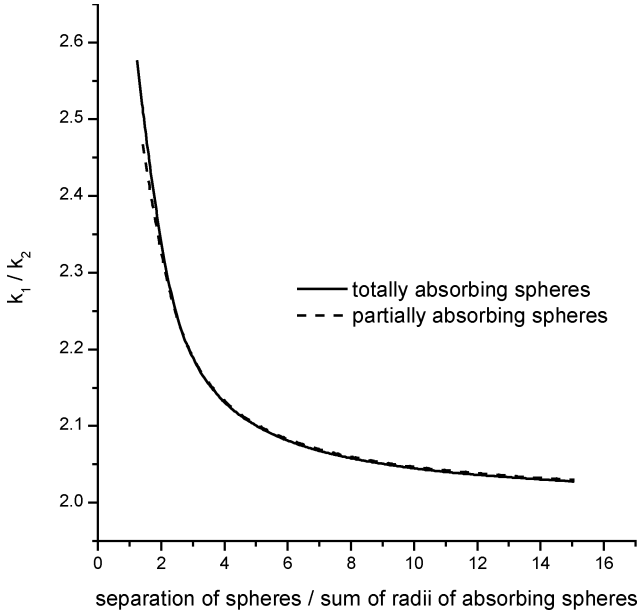

Figure 10. Ratio of reactivity of sphere 1 to sphere 2 as a function of separation. Sphere 1 is twice as reactive as sphere 2 when each sphere is in isolation. This difference in reactivity is accounted for in either of two ways: in the first, both spheres are the same size and have partially absorbing boundaries with reactivity parameters chosen such that sphere 1 is twice as reactive as sphere 2; in the second, both spheres have totally absorbing boundaries and sphere 1 has twice the radius of sphere 2.

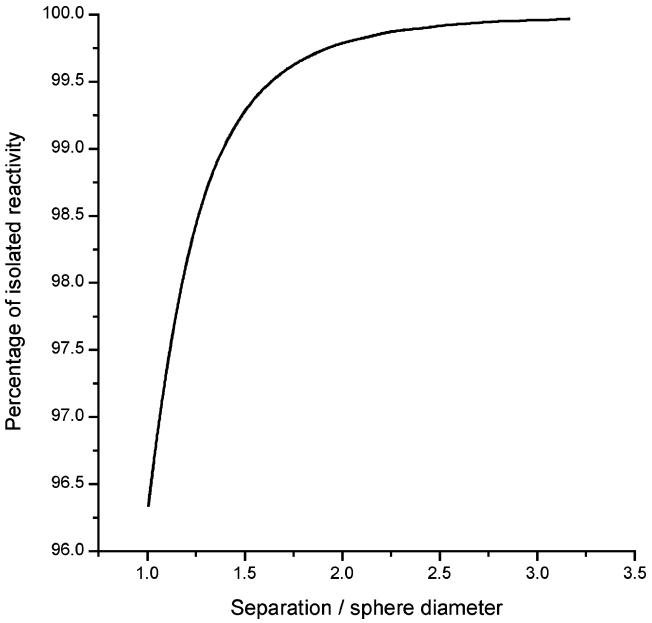

Figure 11. Reduction in relative reactivity of a sphere in the neighborhood of a second unreactive sphere of the same size.

the ratio is significantly greater than the limit at infinite separation, which is two. At separations greater than about 15 spherical diameters, the effect of competition is minimal.

6.2.3. One Absorbing Sphere and One Reflecting Sphere. This Section considers how the rate constant for reaction between the diffusing particle and a totally absorbing sphere is affected by the presence of a totally reflecting adjacent sphere. Figure 11 shows that there is only a slight reduction in the reactivity of the reactive sphere when a reflecting sphere of the same size is almost touching. Beyond a few spherical diameters, the rate constant returns to its value for the isolated sphere. This small effect might be surprising because one would have expected

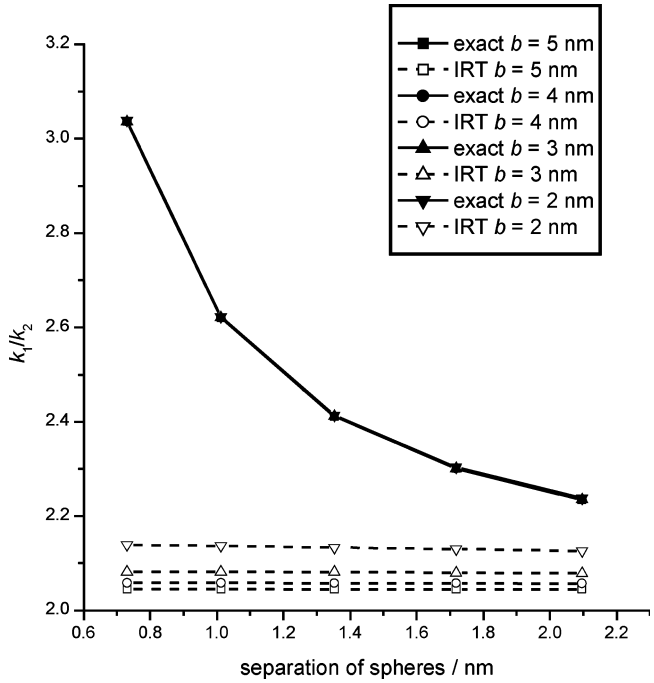

Figure 12. Ratio of rate constants for reaction with sphere 1 to reaction with sphere 2 as a function of the separation of the spheres. The reaction radii for sphere 1 and sphere 2 are 0.40 and 0.20 nm, respectively; both spheres are totally absorbing. The results using the exact solution, eq 17, are independent of b, the radius of the virtual sphere used in the calculation.

the unreactive sphere to shield the reactive one; however, it also reflects trajectories into the reactive sphere, and these effects largely cancel out. This has an important implication where a molecule has a reactive site and unreactive sites. The position of the unreactive site would seem to have little effect on the rate constant for reaction at the active site.

6.2.4. Rate Constants from the IRT Method. Although the IRT method has obviously not proved successful in describing the probabilities of reaction with sphere 1 before sphere 2, it is of interest to test whether the IRT method can give any insight into the competition effect. This is for two reasons: first, the IRT method is often easier to analyze and simulate than the full solution; second, the normal formulation of the rate constant depends on the assumption that the diffusing particles diffuse independently in the frame of reference of the sinks (the independent pairs approximation). The IRT rate constant for reaction with sphere 1 is obtained from the IRT approximation for $\mathscr{P}_1$ averaged over a virtual sphere in the same way as was done for the analytic solution for $\mathscr{P}_1$, described in Section 3.

This calculation is subject to a severe problem. Although the rate constant obtained from the analytic solution for $\mathscr{P}_1$ is independent of the radius of the virtual sphere, the IRT rate constant is not, as shown in Figure 12. The value obtained for the IRT rate constant decreases as the radius of the virtual sphere is increased and seems to approach a limiting value.

Notwithstanding this problem, it is possible to estimate the required IRT rate constant with some choice of sufficiently large virtual sphere, and when this is done the ratio of the rate constants k_1/k_2 does not show any of the competitive effect of the full solution, as illustrated in Figure 12.

It is concluded, therefore, that the IRT method does not recognize the important competition effect that arises when two reactive sites are close to one another and, furthermore, the calculation of a rate constant from analysis of the rate of first

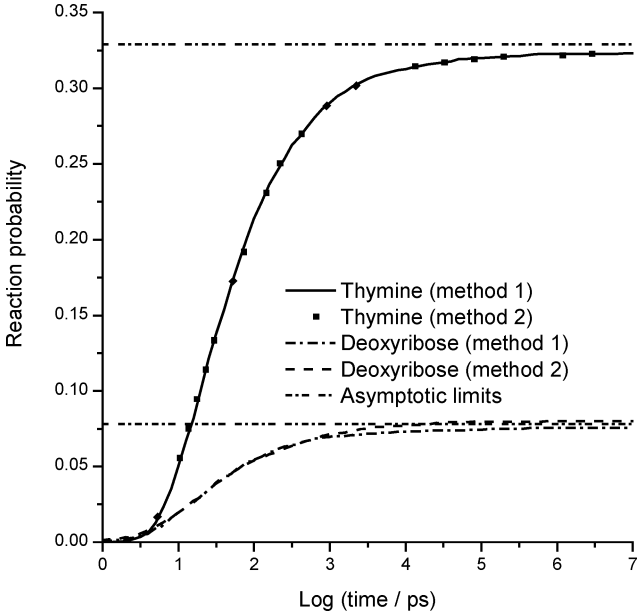

Figure 13. Monte Carlo simulated reaction probabilities for thymine and deoxyribose as components of thymidine. Two methods of treating reactivity are compared. In both methods, thymine is assigned a radius of 2.25 Å and an absorbing boundary. In method 1, deoxyribose is assigned an absorbing boundary with an effective radius of 0.95 Å; in method 2, it is assigned a realistic radius of 1.35 Å with a partially absorbing boundary and a reaction velocity of 0.61 Å ps^{-1}. The horizontal lines are the long-time-limit analytic solutions using a two-sphere model for thymidine.

hitting a virtual sphere and the IRT reaction probability averaged over that sphere is subject to systematic error.

7. Thymidine Application

This Section describes an application of the work presented in this paper. The molecule of interest is the nucleoside thymidine, which consists of a 2′-deoxyribose sugar ring bonded at C-1′ to N-1 of a thymine base. If an aqueous solution of thymidine is irradiated, then the thymine base and the sugar ring of the molecule compete for hydroxyl radicals produced in the irradiation process. The reaction with thymine occurs predominantly by addition at the C5−C6 double bond.[24] OH radicals react with 2′-deoxyribose by abstraction of carbon-bonded H atoms. There are eight of these on the sugar ring, and the selectivity of this reaction is low. The experimental ratio of the rate constants for reaction of OH radicals with the thymine moiety to reaction with the sugar has been found to be about 10:1.[2] By way of comparison, the rate constants for hydroxyl radical reaction with free thymine in water and that with free 2′-deoxyribose are 6.4×10^9 dm^3 mol^{-1} s^{-1} and 2.5×10^9 dm^3 mol^{-1} s^{-1}, respectively, giving a ratio of approximately 2.6:1.[1] This Section investigates the extent to which the dramatic difference between the two ratios may be accounted for in terms of competition between the base and the sugar for OH radicals. The two reactive moieties are modeled as proximal static spherical sinks whose separation and individual radii are determined using crystallographic data.

The first step is to calculate effective reaction radii for both the sugar and the base because it is necessary to factor out the effect of the different diffusion coefficients of the two species. The effective radius may be defined through the equation

$$k = 4\pi\, a_{\text{eff}} D' \tag{64}$$

where k is the rate constant for reaction with OH and D' is the relative diffusion coefficient, that is, the sum of the diffusion coefficients of OH and either the base or sugar. The diffusion coefficient of the OH radical at 25 °C was taken to be 2.8×10^{-9} m^2 s^{-1},[25] and that of thymine was estimated at 25 °C from the literature value[26] at 30 °C using the Stokes−Einstein relationship: a value of 9.5×10^{-10} m^2 s^{-1} was obtained. We were unable to find a literature value for the diffusion coefficient of 2′-deoxyribose, but took as an approximation the diffusion coefficient of D-glucose at 25 °C, that is 6.7×10^{-10} m^2 s^{-1}.[26] Using these diffusion coefficients in eq 64 together with the rate constants shown above, the following values were calculated for the effective reaction radii: thymine, 0.225 nm; 2′-deoxyribose, 0.095 nm. The ratio of effective radii of thymine to 2′-deoxyribose is therefore 2.4:1. The small difference between this and the ratio of rate coefficients is entirely due to the different diffusion coefficients of the thymine and the sugar.

The question is whether the ratio of attack by OH at each of these two species when bonded together in thymidine remains close to the value of 2.4:1 or whether the effects of competition increase the ratio toward the experimentally determined ratio of 10:1.

7.1. Analytic Investigation. Using the method of Section 2.3, thymine and deoxyribose were modeled as totally absorbing spheres of radii 0.225 and 0.095 nm, respectively. In accordance with the crystallographic data for thymidine,[27] their centers were placed 0.36 nm apart, being the distance between the center of the C5−C6 bond of thymine and the centroid of deoxyribose. Using the method of Section 3, a rate constant was found for each of the two reactive sites on thymidine and their ratio was found to be 4.2:1 in favor of thymine, showing that the competitive effect results in a substantial increase of this ratio.

The same investigation was carried out on the assumption that the reaction of OH with thymine is fully diffusion-controlled but that that with deoxyribose is partially diffusion-controlled. The method of Section 2.5 was used with a radius for thymine of 0.225 nm and for deoxyribose a radius of 0.135 nm and a reaction velocity of 61 m s^{-1} were assumed. The radius chosen for deoxyribose is the largest value consistent with the crystallographic data where the two spheres do not overlap because the bispherical coordinate system does not permit overlap of spheres of constant μ. The reaction velocity relates the effective radius to the actual radius through the equation[8]

$$a_{\text{eff}} = \frac{a}{1 + D'/\nu a} \tag{65}$$

The velocity of 61 m s^{-1} assigned to the reaction between the OH radical and deoxyribose ensures that eq 65 leads to the correct effective radius for free deoxyribose, 0.095 nm. The ratio of effective radii for thymine and deoxyribose in thymidine was found to be 4.1:1 by this method, very similar to the situation where effective radii were used.

It is apparent from the above discussion that arguments based on the competition of the two reactive moieties in thymidine do not completely explain the dramatic favoring of the OH−thymine reaction over the OH−sugar reaction in thymidine. However, it does account for some of the increase, suggesting a rise in the ratio from 2.4:1 to just over 4:1. It should be remarked, though, that had it been possible to analyze the case where the spheres representing thymine and deoxyribose overlap, a ratio closer to the experimental value of 10:1 might have been found. The crystallographic data reveals that a more appropriate model would be one where the imaginary spheres enclosing each of the two reactive moieties overlap and are truncated where they meet. This system could be solved exactly

using the toroidal coordinate system because this allows for a degree of overlap between the reactive spheres. Work is in progress.

It might also be more appropriate to model the reactive sites on the deoxyribose separately. This cannot be done within the bispherical coordinate system because it requires eight spheres. More detailed models such as this may, however, be amenable to simulation by the Monte Carlo random flights method.

7.2. Simulation Method. This Section describes the random flights simulation of the reaction between an OH radical and an aqueous solution of thymidine, to deduce a rate constant for reaction with either the sugar or the base. The details of the simulation method have been discussed elsewhere,[17,28−30] and only a brief discussion is given here.

An OH radical is placed at a random point on the surface of a virtual sphere that completely encloses the thymidine molecule. The diffusion of the radical in the aqueous medium containing the thymidine molecule is simulated by identifying its location at a sequence of time steps. The distance traversed in each of three mutually orthogonal directions in time step δt is a random number drawn from a spherical normal distribution with mean zero and variance $2D\delta t$. If the OH radical encounters a reactive sphere during δt, then a reaction is counted. Encounter is determined in two ways: either the radical is found to overlap with an atom at the end of the time step or the probability is calculated for the radical to have reacted during the time step, even though there is no overlap at the end of the time step.[29] The simulation continues until the OH radical has reacted or until a given cutoff time has elapsed. The whole process is repeated several thousand times allowing time-dependent reaction probabilities to be calculated. At each new realization, the OH radical starts at a different random point on the surface of the virtual sphere. In this way the probability of reacting with each moiety is averaged over the virtual sphere. The rate constants for reaction with both the sugar ring and the thymine base are then calculated in accordance with the method of Section 3.

The same system has been simulated to verify the analytical results described above. The simulation has the added advantage of giving a time-dependent reaction probability. Figure 13 shows the time-dependent reaction probabilities from such a simulation, together with the asymptotic limits calculated using the analytic methods described in Section 2. Figure 13 shows the system modeled with two absorbing spheres with effective radii, and with two realistic spheres, as discussed above, with a partially absorbing boundary condition. It can be seen that the time dependence in these two models is very similar.

Although the analysis described in this paper can only be performed for two nonintersecting spherical sinks, simulations are not limited in this way, and it is clearly of interest to investigate whether the competition effect is enhanced by considering the reactivity of the two moieties at a finer level. For this purpose each atom in deoxyribose is modeled as a sphere of appropriate size whose center is in accordance with the crystallographic data. The encounter radius of a sphere is assumed to be the sum of the covalent radius of the atom and half the OH−OH encounter distance. The latter was obtained using the rate constant for the combination of two OH radicals using eq 64. In addition, a sphere of radius 0.225 nm is placed at the center of the C5−C6 bond to represent the reactive part of the thymine molecule. Unreactive atoms can either be ignored or included explicitly. If the radical encounters an unreactive atom during δt, then it is reflected from that atom using a standard procedure.[23]

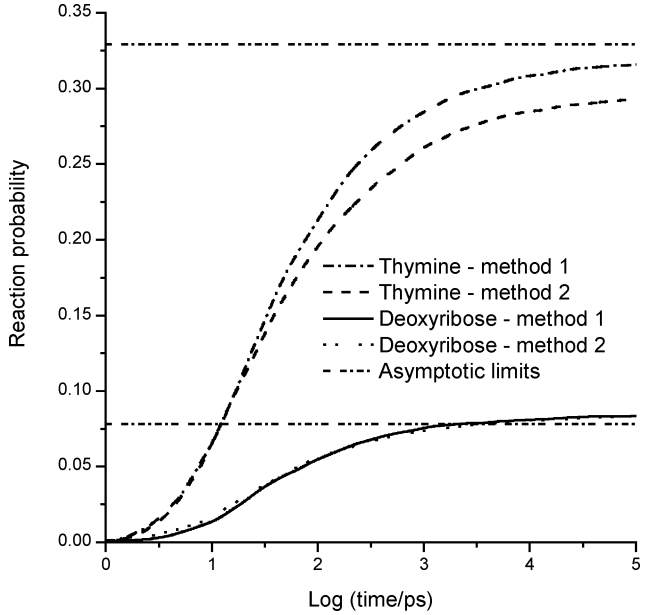

Figure 14. Monte Carlo simulated time-dependent reaction probabilities of thymine and deoxyribose as components of thymidine using an atomistic model. Two methods of treating unreactive atoms are compared: in method 1, unreactive atoms of deoxyribose are excluded; in method 2, unreactive atoms are included. The horizontal lines are the long-time-limit analytic solutions using a two-sphere model for thymidine.

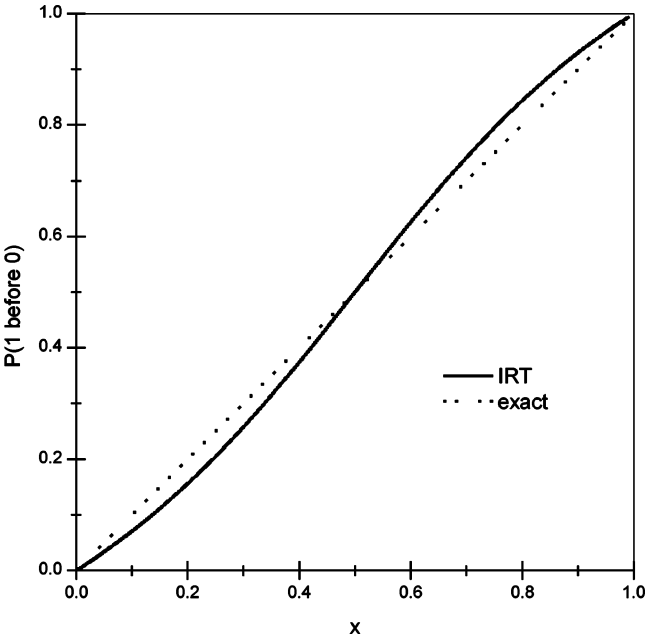

Figure 15. One-dimensional diffusion of a particle starting at $X = x$ with absorbing boundaries at $X = 0$ and $X = 1$. The plot shows the probability of hitting the upper boundary first calculated by (1) the IRT method and (2) the exact method.

The reaction velocity of each reactive (carbon-bonded) H atom in deoxyribose was found by a method of *trial and improvement*. The simulation was carried out on deoxyribose alone (i.e., ignoring thymine) using the appropriate reaction radii. Each reactive H atom was assumed to have the same reaction velocity, and a realistic velocity was assigned. The simulation was run with this trial velocity, and a rate constant for the OH reaction with deoxyribose was calculated on the basis of the results. This was compared with the experimental rate constant. The simulation was repeated with a different trial velocity in order to better reproduce the known rate constant. Further

simulations were run using other trials until the simulated rate constant was arbitrarily close to the experimental value. The reaction velocity assigned using this method was 7 m s^{-1} when *all* atoms of deoxyribose were included and 3.6 m s^{-1} when only the reactive atoms were included.

This model is obviously still crude and could be refined further. For example, it is known that the reactive C−H bonds in deoxyguanosine have substantially different bond dissociation energies,[31] and this will clearly have an effect on the appropriate reaction velocities. In addition, in the thymine moiety there is significant preference for attack on C5 rather than C6 or H abstraction.[32]

The results of these simulations are shown in Figure 14. The yield of reactions with deoxyribose is not dependent on whether the unreactive atoms are included in the simulation, and the exact result for the two-sphere model is acceptable for this yield. However, there is more variation in the yield of reaction with the thymine moiety. Including the unreactive atoms reduces the yield of this reaction. Presumably the thymine is being shielded by the umbrella of the sugar molecule. The ratio of the reactivity of the two moieties is 3.5 when the unreactive atoms are included and 3.8 when they are not. Agreement with experiment is worse for these more detailed models than for the simple two-sphere model.

The simulation method can also be applied to the two-sphere model where the spheres intersect. However, this application raises new technical difficulties because of the intersection of the boundaries. In particular, it is necessary to develop an unbiased method of estimating which sphere is attacked when it is possible to attack both in the same time-step of the simulation. This is never a problem with nonintersecting targets because it is always possible to make the step small enough that it only has a significant probability of attack on one sphere. Work on this boundary problem is in progress and we hope to report an efficient method shortly.

It seems clear that there is an important competition effect between the sugar and the thymine but that this is not sufficient to explain the large preference for thymine in the experiments.

8. Conclusions

This paper has presented an exact solution for the probability that a diffusing particle will hit one sphere before another in a system containing two fixed spherical sinks. The solutions have been presented for the case of totally absorbing spheres, using a Smoluchowski boundary condition, and for partially reflecting spheres using a radiation (elastic) boundary condition. Solutions for the steady-state rate constants for hitting either sphere have also been investigated. In addition, the applicability of the IRT method to such systems has been tested.

When the spheres are close to one another, an important competition effect has been found in which each sphere shields reactivity from the other; that is, the effective reactivity of each sphere is reduced by the proximity of the other sphere. One important result is that the reactivity of the total system is less than the sum of the reactivities of the two spheres in isolation. This is potentially an important consideration when comparing the reactivities of two proximate moieties in the same molecule. When the two spheres have different intrinsic reactivities, the less reactive sphere is affected more by the competition than the more reactive sphere. This competition effect is not significantly affected by the use of "effective" reaction radii to allow for deviations from full diffusion control.

The IRT method was found not to recognize this competitive effect at all and so cannot be considered reliable for systems that contain two proximate reactive centers, either for the total reaction rate or for its division between the centers. In addition, the rate constants obtained by the IRT method were found to depend on the radius of the virtual sphere used in the calculation.

The analysis was applied to thymidine, where the differentiation between the reactivities of the sugar and the base to OH radicals is much more pronounced than would be expected from the published rate constants for OH + thymine and OH + deoxyribose. It was found that although the competition effect does result in a substantial increase of the relative reactivity of the base, this was not sufficient to explain the whole experimentally observed effect. Because of the simplicity of the two-sphere model a more realistic model of thymidine was also considered using Monte Carlo random flights simulations, but a similar and slightly worse result was obtained.

The analysis in this paper is limited to two nonoverlapping spheres because of the coordinate system used, and in addition it ignores any possible rotational motion of the entity containing the reactive sinks. Further work is in progress to relax these approximations.

Appendix: One-Dimensional IRT versus Exact Analysis

Section 6.1.2. discussed the accuracy of the IRT method in calculating the probability of a diffusing particle hitting one absorbing sphere before the other from a point outside. The results for a particle initially at a point along the line of centers and between the spheres were presented, and the ratio between the probability as calculated by the IRT method and the exact solution was calculated. To facilitate an understanding of this ratio when the particle starts at a point between the two spheres, the simpler problem of one-dimensional diffusion is considered here. Although it is unlikely that a radical can be generated between the two targets in a molecule such as thymidine, if the sinks are on a larger scale, such as the strands of a DNA molecule, or even two planes, such behavior might be of interest.

Consider a diffusing particle confined to the x axis whose position at time zero is $X = x$, where $a < x < b$. There are absorbing boundaries at $X = a$ and $X = b$. The probability that the particle hits the boundary at $X = b$ before that at $X = a$ is required. The calculation is first carried out using the IRT method. In this approximation, the first passage times to hit a and b are generated independent of one another but conditional on the distances from the initial position to each boundary, and the decision about which boundary is hit first depends only on which of these times is smaller. This is equivalent to starting two independent trajectories simultaneously from the point x. One of these targets the boundary at $X = a$ and may be killed only upon reaching this point regardless of whether it hits b first; the other targets the boundary at $X = b$ and, likewise, is killed at no other point. According to the IRT methodology, whichever trajectory reaches its target first registers a hit at that boundary.

Consider first the trajectory that targets the boundary at $x = b$. Let T_b be the time at which it hits this boundary for the first time, then the probability distribution function for T_b is

$$P(T_b < t_b) = \mathrm{erfc}\left(\frac{b-x}{\sqrt{4Dt_b}}\right) \tag{66}$$

The density of the time at which this boundary is hit is the time derivative of the distribution function is as follows:

$$p(t_b) = \frac{b-x}{\sqrt{4\pi\, Dt_b^3}} e^{-(b-x)^2/4Dt_b} \tag{67}$$

There are equivalent equations for the distribution function and density function of the time at which the boundary at $X = a$ is first hit by its trajectory. The IRT probability that the boundary at $X = b$ is hit first is therefore given by

$$P(T_a > T_b) = \int_0^\infty \frac{b-x}{\sqrt{4\pi\, Dt_b^3}} e^{-(b-x)^2/4Dt_b} \operatorname{erf}\left(\frac{x-a}{\sqrt{4Dt_b}}\right) dt_b \tag{68}$$

By making the substitution

$$u = \frac{1}{\sqrt{4Dt_b}}$$

the integral becomes

$$P(T_a > T_b) = \frac{2(b-x)}{\sqrt{\pi}} \int_0^\infty e^{-(b-x)^2u^2} \operatorname{erf}((x-a)u)\, du \tag{69}$$

With the substitution $y = (x - a)u$, this becomes

$$P(T_a > T_b) = \frac{2(b-x)}{\sqrt{\pi}(x-a)} \int_0^\infty e^{-(b-x)^2y^2/(x-a)^2} (1 - \operatorname{erfc} y)\, dy \tag{70}$$

The integral is now in a standard form whose solution[20] is

$$P(T_a > T_b) = \frac{2}{\pi} \tan^{-1} \frac{x-a}{b-x} \tag{71}$$

The exact solution is trivially found by solving the steady-state backward equation with appropriate boundary conditions to give

$$P(T_a > T_b) = \frac{x-a}{b-a} \tag{72}$$

Figure 15 shows the IRT and exact solutions when the boundaries are at $a = 0$ and $b = 1$. It is seen that the IRT method overestimates the probability of hitting b first if the particle starts nearer b than a but underestimates the same probability if the particle starts nearer a than b. Figure 16 shows the ratio of the IRT solution to the exact solution. This is very similar in behavior to the three-dimensional equivalent in Figure 7.

To justify, in a physical sense, the shape of the IRT curve in Figure 16, consideration has been given to every permutation of hitting points and times in which two independent trajectories may evolve for a diffusing particle that starts at a point between a and b. Each trajectory will ultimately hit both boundaries and so there are four first hitting times, two for each trajectory. The graphs in Figure 17 illustrate every possible ordering of these hitting times; increasing time is designated by the downward direction. There are 12 possible permutations, and these are illustrated in Figure 17.

In the exact analysis, each of the two trajectories registers a hit on either a or b, depending on which of these two boundaries is hit first. In the IRT method, whichever trajectory reaches its own target first registers a hit on that target; the other trajectory is then ignored in the analysis. Earlier hits on the wrong boundary are also ignored. Thus, for example, the first permutation registers two hits on a by the exact method because each trajectory hits a before it hits b. The IRT method registers a single hit on a or a single hit on b depending on which of the two trajectories is designated as being a-seeking and which as b-seeking because one trajectory hits both a and b before the other hits anything. The labeling beneath each permutation in Figure 17 shows how each is interpreted by, first, the exact analysis and, second, by the IRT method with each possible labeling of the two trajectories.

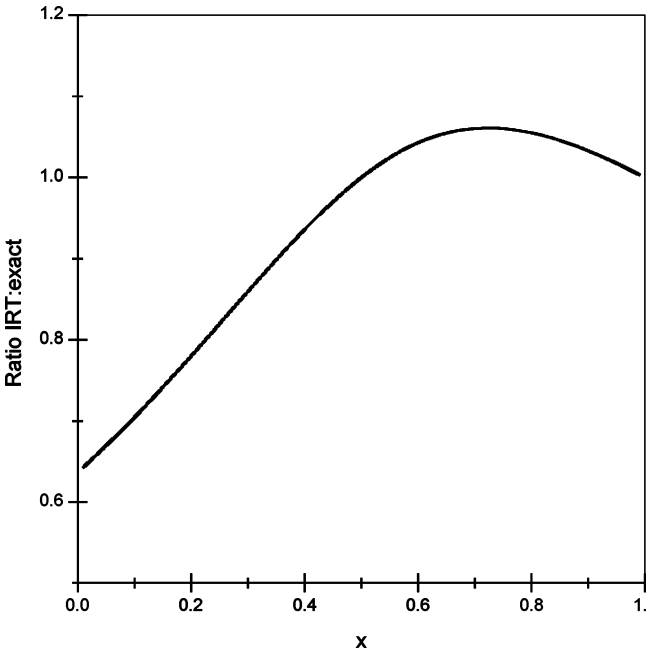

Figure 16. One-dimensional diffusion of a particle starting at $X = x$ with absorbing boundaries at $X = 0$ and $X = 1$. The plot shows the ratio of the IRT solution to the exact solution for the probability of hitting the upper boundary first.

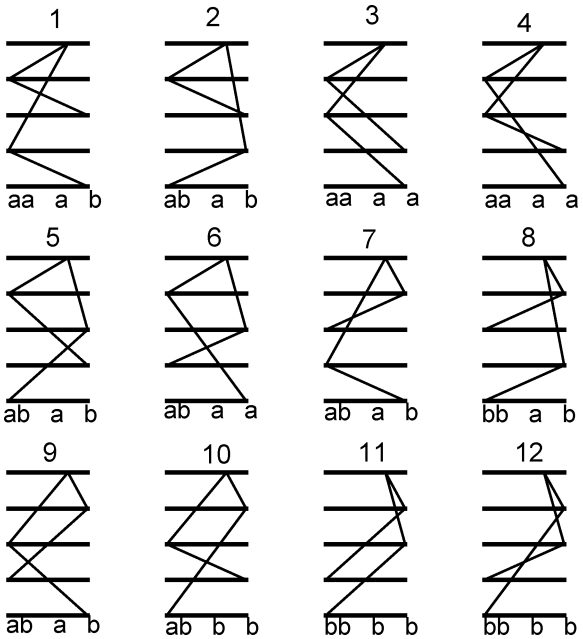

Figure 17. Scheme showing all possible ways in which two independent trajectories may develop in time from a starting point three-quarters of the way along the line between two absorbing boundaries at a and b. The first pair of letters beneath each figure shows the allocation of hits according to the exact method; the second pair shows the IRT interpretation.

It is of interest that in all but four of the permutations, the two interpretations are identical. Of the remaining four, numbers 1 and 10 overstate the number of hits on b in the IRT analysis while numbers 6 and 8 understate this number. Whether the IRT method overestimates or underestimates the probability of

hitting *b* first depends on the relative likelihood of these four permutations.

This problem was addressed by simulating the evolution of two independent trajectories starting simultaneously at a point three-quarters of the way along the *x* axis from *a* to *b*. The simulation generates a random time for each trajectory to hit either boundary for the first time and then a subsequent random time to hit the other boundary starting from the first. It then records the order in which boundaries were first hit by each of the pair of trajectories. The simulation was repeated 1 million times and the relative number of occasions each permutation arose was determined. Numbers 9, 10, 11, and 12 accounted for 83% of all permutations. In particular, number 10 accounted for 14%, while numbers 8, 6, and 1 accounted for 2%, 3%, and less than 1%, respectively. Thus, the overriding consideration is the overstatement of the number of hits on *b* when the sequence of events illustrated in permutation 10 occurs. This confirms that the IRT method overestimates the probability of hitting boundary *b* when the particle starts at a point three-quarters of the way toward *b* on the straight line between *a* and *b*.

By symmetry, for a particle starting closer to *a* than *b* the IRT method will overestimate hits on *a* because of the large fraction of trajectories of type 6.

Acknowledgment. We acknowledge the financial support of EPSRC for this research. We would also like to thank a referee for pointing out references 31 and 32.

References and Notes

(1) Buxton, G. V.; Greenstock, C. L.; Helman, W. P.; Ross, A. B. *J. Phys. Chem. Ref. Data* **1988**, *17*, 513.
(2) von Sonntag, C. Private communication.
(3) Samson, R.; Deutch, J. M. *J. Chem. Phys.* **1977**, *67*, 847.
(4) Sano, H. *J. Chem. Phys.* **1981**, *74*, 1394.
(5) Karlin, S.; Taylor, H. M. *A Second Course in Stochastic Processes*; Academic Press: New York, 1981.
(6) Morse, P. M.; Feshbach, H. *Methods of Theoretical Physics*; McGraw-Hill: New York, 1953; pp 665 f, 1298 ff.
(7) Collins; F. C.; Kimball, G. E. *J. Colloid Sci.* **1949**, *4*, 425.
(8) Green, N. J. B. *Mol. Phys.* **1986**, *58*, 145.
(9) Steinberg, J. Z.; Katchalski, E. *J. Chem. Phys.* **1968**, *48*, 2402.
(10) Gosele, U. *Chem. Phys. Lett.* **1980**, *69*, 332.
(11) Tachiya, M. *Radiat. Phys. Chem.* **1983**, *21*, 167.
(12) Green, N. J. B. *Chem. Phys. Lett.* **1984**, *107*, 485.
(13) Bleaney, B. I.; Bleaney, B. *Electricity and Magnetism*; Clarendon Press: Oxford, 1963.
(14) Yennie, D. R.; Ravenhall, D. G.; Wilson, R. N. *Phys. Rev.* **1954**, *95*, 500.
(15) Hardy, G. H. *Divergent Series*; Clarendon Press: Oxford, 1949.
(16) Clifford, P.; Green, N. J. B.; Pilling, M. J.; Pimblott, S. M.; Burns, W. G. *J. Chem. Soc., Faraday Trans. 1* **1984**, *80*, 1313.
(17) Green, N. J. B.; Oldfield, M. J.; Pilling, M. J.; Pimblott, S. M. *J. Chem. Soc., Faraday Trans. 1* **1986**, *82*, 2673.
(18) Green, N. J. B.; Pilling, M. J.; Pimblott, S. M.; Clifford, P. *J. Phys. Chem.* **1990**, *94*, 251.
(19) Pimblott, S. M.; LaVerne, J. A. *J. Phys. Chem.* **1997**, *101*, 5828.
(20) Gradshteyn, I. S.; Ryzhik, I. M. *Table of Integrals, Series, and Products*; Academic Press: New York, 1980.
(21) Rice, S. A. *Comprehensive Chemical Kinetics*, vol. 25; Elsevier: Amsterdam, 1985.
(22) Clifford, P.; Green, N. J. B.; Pilling, M. J. *J. Phys. Chem.* **1982**, *86*, 1322.
(23) Pimblott, S. M.; Green, N. J. B. *J. Phys. Chem.* **1992**, *96*, 9338.
(24) von Sonntag C. *The Chemical Basis of Radiation Biology*; Taylor and Francis, London, 1987.
(25) LaVerne, J. A.; Pimblott, S. M. *J. Phys. Chem.* **1991**, *95*, 3196.
(26) Nishida, K.; Ando, Y.; Kawamura, H. *Colloid. Polym. Sci.* **1983**, *261*, 70.
(27) *www.ccdc.cam.ac.uk*
(28) Clifford, P.; Green, N. J. B.; Pilling, M. J. *J. Phys. Chem.* **1985**, *89*, 925.
(29) Green, N. J. B. *Mol. Phys.* **1988**, *65*, 1399.
(30) Green, N. J. B.; Pilling, M. J.; Pimblott, S. M. *Radiat. Phys. Chem.* **1989**, *34*, 105.
(31) Steenken, S.; Jovanovic, S. V.; Candeias, L. P.; Reynisson. J. *Chem.—Eur. J.* **2001**, *7*, 2829.
(32) von Sonntag, C. *Free-Radical Induced DNA Damage and its Repair. A Chemical Perspective;* Springer-Verlag: Berlin, Germany, 2006.